

# Numerical simulations of the formation behavior of explosively formed projectiles

Minel Salkičević\*

<sup>1</sup> Defense Technologies Department, Mechanical Engineering Faculty, University of Sarajevo

\* Corresponding author E-mail: [s.minel97@gmail.com](mailto:s.minel97@gmail.com)

Received Oct. 13, 2021

Revised Dec. 22, 2021

Accepted Jan. 12, 2022

## Abstract

Explosively formed projectile (EFP) is a self-forging shape charged structure having very high penetration ability compared to conventional kinetic energy projectile. The penetration capability of an EFP is strongly dependent on various design parameters. The main parameters can be roughly divided into geometric and material parameters used in the warhead configuration.

The present research is an effort to study the effect of metal casing thickness, type of metal used for casing, explosive type, liner thickness, type and configuration on the formation of EFP. Effectiveness of an EFP is studied in terms of final velocity and shape of formed penetrator. The study is carried out by performing a number of simulations by using explicit finite element (FE) hydrocode ANSYS/Autodyn.

© The Author 2022.  
Published by ARDA.

**Keywords:** Explosively formed projectiles (EFP); Numerical Simulations; ANSYS/Autodyn

## 1. Introduction

Generally, an explosively formed projectile system consists of charge, liner, casing and wave-shaper. The geometric and physical parameters like length, diameter, liner shape and material and type of charge strongly influence the shape and velocity of the penetrator [1].

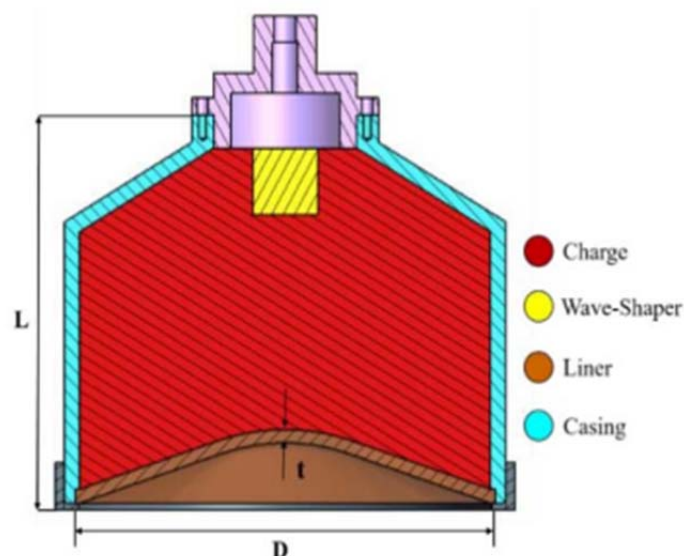


Figure 1. The schematic of EFP configuration [1]

Similar to shaped charge (cumulative) projectiles, after detonation, very high pressure collapses the liner into the appropriate shape (depending on the design) of the penetrator moving at a speed of up to 3 km/s [2]. The process of penetrator formation from the initial shape of the liner is shown in Figure 2 [3].

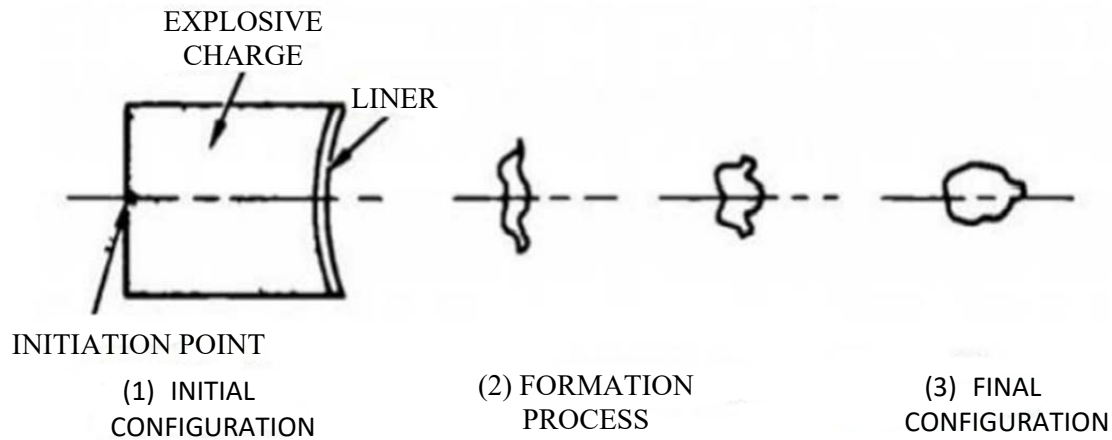


Figure 2. The formation process of EFP [3]

There are two structural types of solutions used in the fight against armored combat vehicles. The first type are anti-tank penetrating mines (with antenna or non-contact, electromagnetic activation mechanism), effective at a distance of up to one meter – one such is shown in Figure 3a. The second type are explosively formed projectiles that are used to pierce armor at greater distances (stand-off projectiles) – shown in Figure 3b. The penetrating abilities of these two types are different, which results from the way of attacking the chosen target. The first type hits the floor plate or tracks of an armored vehicle (in modern tanks, the floor armor is not thicker than 20 mm). The second type hits the side armor (the thickness of the side armor in modern tanks does not exceed 80 mm), and in modern times also the upper side of the tank armor. The minimum penetrating power of the first type is 40 mm at a distance of up to one meter, and the second type - 80 mm at a distance of up to 100 m [4].

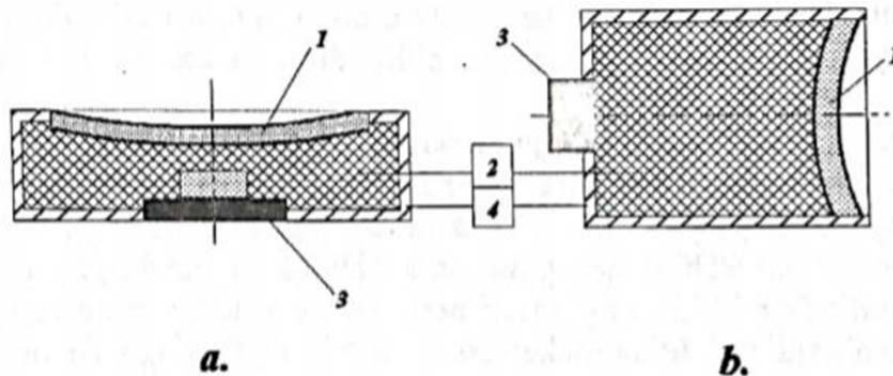


Figure 3. Schematic representation of the solution based on the Misznay Schardin effect (a anti-tank mine; b-EFP; where: 1-liner, 2-exp. charge, 3- activation mechanism, 4-metal casing) [4]

Two major applications have evolved since 1975 for EFP warheads, namely, long-standoff sensor-fuzed submunitions and medium-standoff, close-overflight missiles, as depicted in figure 4. The former application, which is the more traditional one, requires the formation of a single-piece EFP capable of flying in a stable position to the target. This refinement has led to the flared EFP rod and, more recently, to the finned EFP rod designs. For the medium – or short-standoff applications, a new type of EFP was developed. The need for an aerodynamic shape is not necessary for these applications because of the short distance the EFP must travel, hence, the length of the rod was increased and the flared tail was eliminated from the design. In fact, some of these rods are purposely stretched beyond their breaking point and fracture into several pieces resulting in greater total length [5].

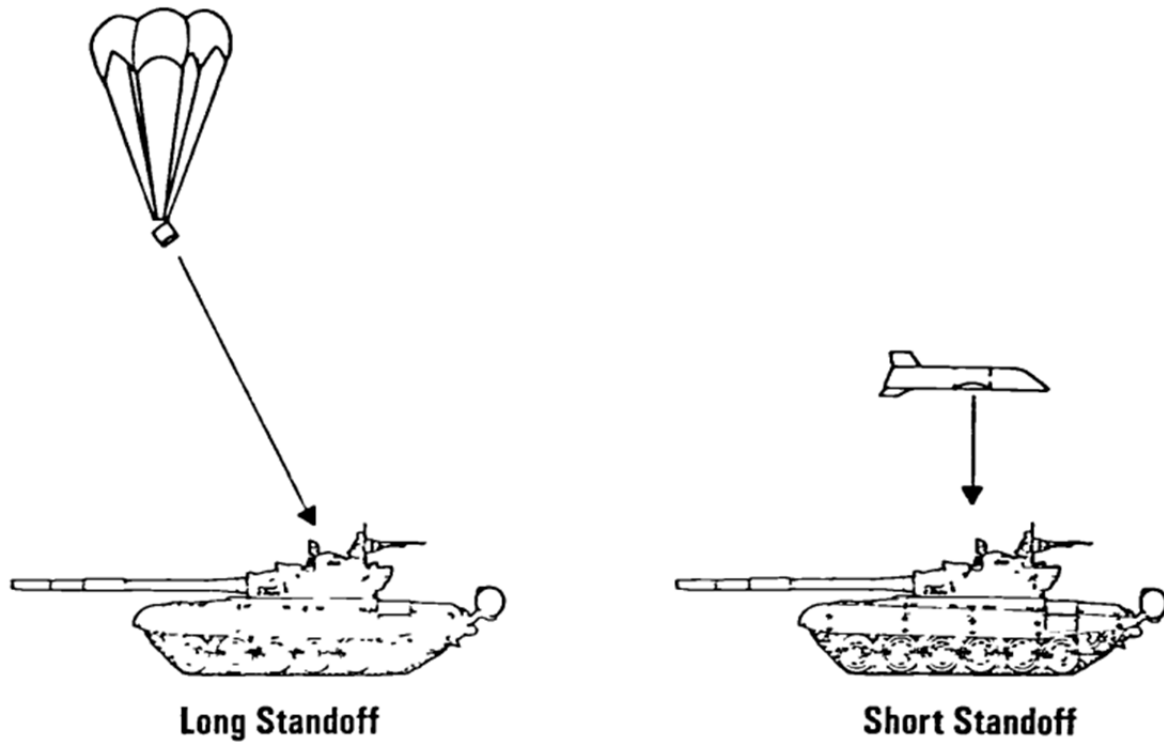


Figure 4. Two modern applications of EFP technology [5]

## 2. Numerical model

The numerical model for simulations are generated using ANSYS/Autodyn software with appropriate boundary conditions and accurate geometric modeling. In order to predict behaviour of the liner, Euler grid is used to design all three components: the explosive, the liner and the casing geometry. The mesh is modelled using 0.25 mm rectangular cells in both regions (the jet formation and the transition region). The free space is filled with still air with an initial density of  $0.001225 \text{ mg/mm}^3$  and internal energy of  $2.06640 \cdot 10^5$  micro-Joules. Outflow boundary condition is applied to all computational borders except the symmetry. This allows the expanding detonation products to leave the computational domain without interacting with its boundaries. Figure 5. shows the initial geometry of standard EFP used in numerical simulations in this paper. [6]

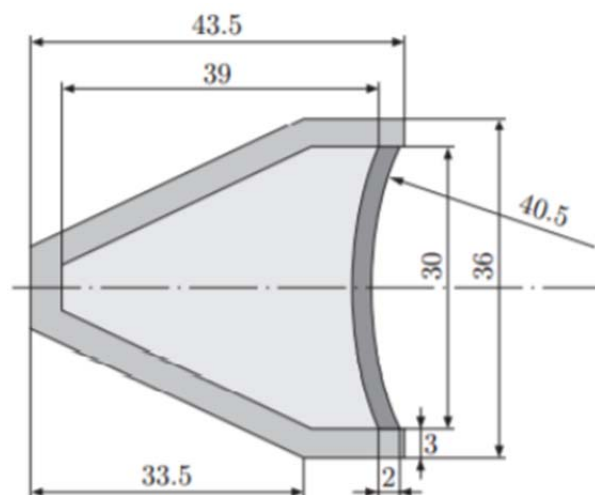


Figure 5. Geometry of simulated EFP [7]

The initial geometry used in this investigation is shown in Fig.6. The HMX was used as exp. charge material. The shaped charge liner is made of copper with different forms and casing is made of steel. It is important to mention that the configurations and materials of previously mentioned parts varies with the test cases. [8]

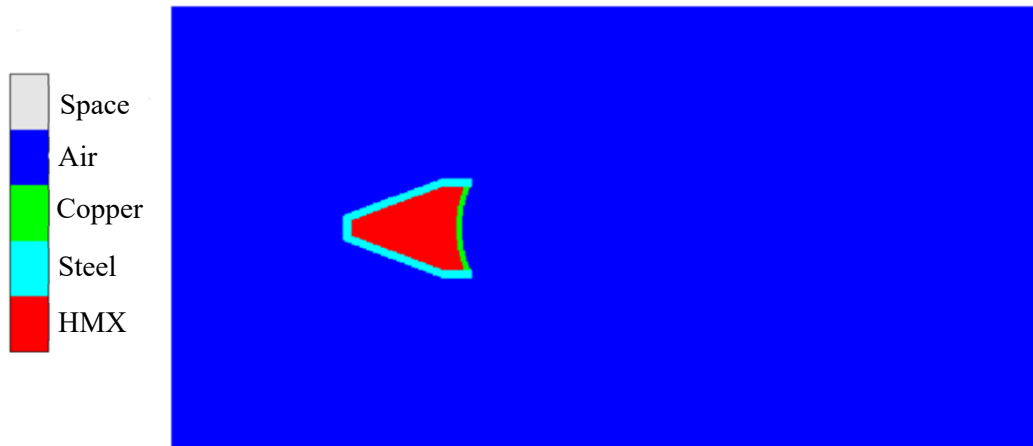


Figure 6. EFP model used in the research (Autodyn) [8]

### 3. Results and discussions

In order to validate numerical model, a series of numerical simulations have been carried out. Obtained results were compared with numerical results found by Hussain et al, [7] where a good agreement was observed.

#### 3.1. Metal casing

In this section, the influence of the metal casing wall thickness and the influence of the metal casing material will be analyzed. Initial configuration is shown in Figure 5. In order to show the influence of metal (steel 4340) casing thickness on the process of penetrator formation, two numerical simulations were performed in the Autodyn software. The configuration of the EFP is the same in both simulations, only the thickness of the metal casing is varied. The thickness in the first simulation is 3 mm (Figure 7a). In the case of the second simulation, the thickness of the metal casing is 5 mm (Figure 7b). [8]

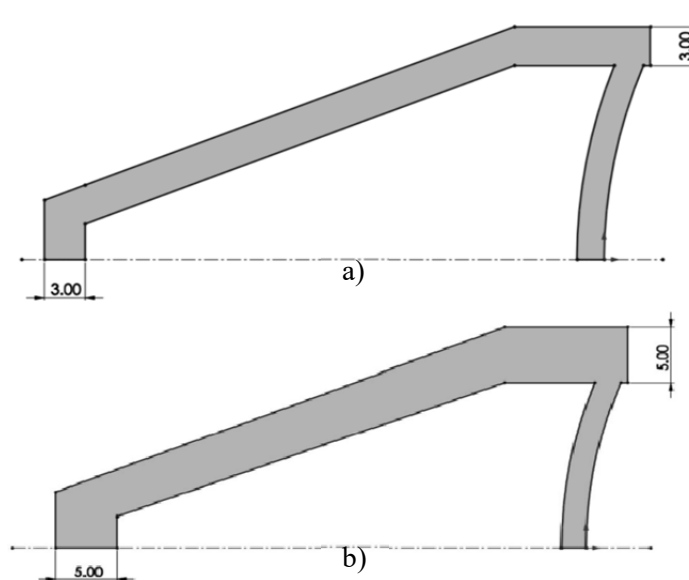


Figure 7. Different metal casing thicknesses used in numerical simulations (Solidworks) [8]

Figure 8 shows formed copper penetrators, as well as their velocities after 100  $\mu$ s. It can be concluded that the thickness of the metal body affects the velocity of the formed penetrator - thicker casing corresponds to a higher velocity of the penetrator. In the case of the first simulation, the casing thickness was 3 mm and the penetrator velocity was about 1750 m/s (Figure 8 - left). In the second simulation, the casing thickness was 5 mm, and the penetrator velocity was about 116 m/s higher than in the first simulation. The thicker the metal casing, around the explosive charge and the liner, the bigger the impact time of the explosive impulse and the bigger the total energy transmitted from the explosive to the liner. [8]

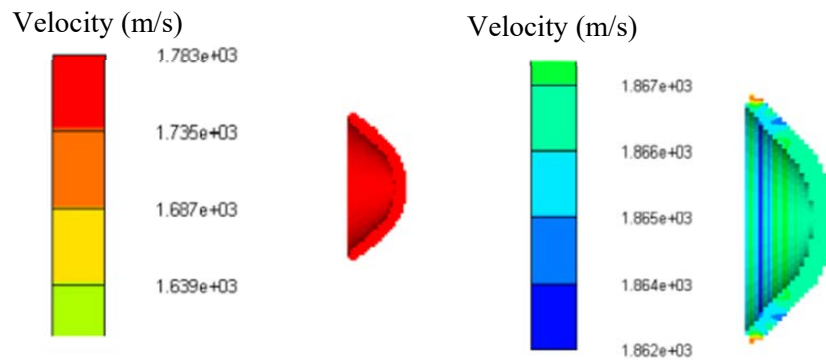


Figure 8. Different penetrator velocities for different metal casing thicknesses (Autodyn) [8]

Apart from the fact that body thickness has an influence on the process of penetrator formation in EFP, it is important to note that the body material also has a certain influence. So another simulation was done that shows the difference between the formed penetrators in the case of a steel casing and a casing made of aluminum. Namely, the geometry of the EFP from Figure 7a was used in the additional simulation. All the characteristics remained the same except that in the additional simulation, aluminum was used as the EFP casing material instead of steel (Figure 9). [8]

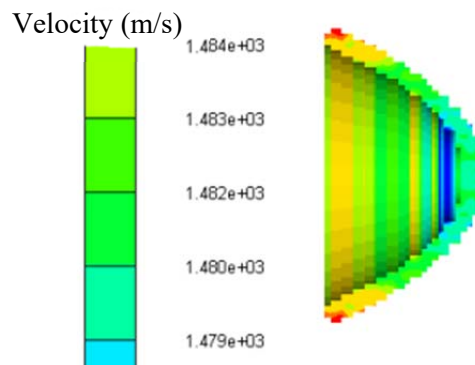


Figure 9. Penetrator velocity of EFP with casing made of aluminum (Autodyn) [8]

In Figure 9 it can be seen that the velocity of the penetrator, in the case of an aluminum casing, is about 1480 m/s. If this velocity is compared to simulation in which the casing was made of steel, it can be concluded that in that case the penetrator had a higher velocity, by about 270 m/s. Material of higher density and higher values of yield strength increases the time of influence of the explosive impulse and increases the total energy transmitted from the explosive to the liner. [8]

Table 1 shows the characteristics of the materials used (steel and aluminum), as well as the difference in penetrator velocities after 100  $\mu$ s ( $t=100 \mu$ s). [8]

Table 1. Characteristics of materials used for EFP's casing and their influence on penetrator velocity [8]

Casing material	Density (kg/m <sup>3</sup> )	Tensile strength (MPa)	Yield strength (MPa)	Penetrator velocity (m/s)
Steel	7830	745	470	1750
Aluminium	2700	305	215	1480

It is also important to note that it is not always possible to choose a material with more favorable characteristics, due to limiting factors. Steel, as a material with higher density than aluminum, increases the overall system mass - which can be a limiting factor. [8]

### 3.2. Explosive charge

In this part, an analysis of the influence of explosive charge type on velocity of the formed penetrator will be performed, and a comparison will be made for the following three types of explosives: HMX, TNT and Comp B. In order to show the influence of the density and other characteristics of explosive charge on the process of penetrator formation, three more numerical simulations are presented below. Initial configuration shown in Figure 5 is retained (all measures, metal casing material – steel 4340, liner material – copper, metal casing

thickness = 3 mm, liner thickness = 2 mm); however now the explosive charge is different (everything else is identical). Instead of the previously used HMX, now a TNT is used, with a lower density and therefore a lower detonation velocity (relative to HMX). [8]

Figure 10 shows a penetrator, initiated by TNT, moving at a velocity of about 1380 m/s. Thus, the same EFP configuration with different explosive charge led to the conclusion that the penetrator velocity was higher by about 370 m/s in the case when octogen (HMX) was used as the explosive charge. [8]

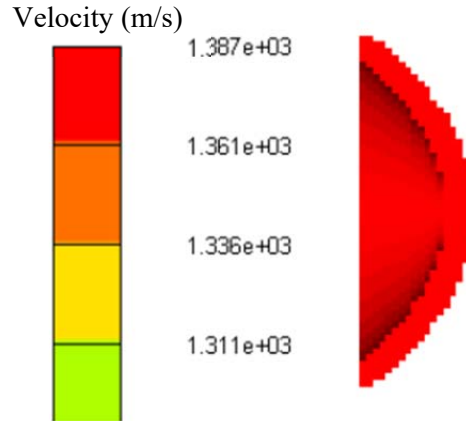


Figure 10. Penetrator velocity of EFP initiated by TNT, measured after 100  $\mu$ s (Autodyn) [8]

Figure 11 shows a penetrator, initiated by composition B, moving at a velocity of about 1635 m/s. The velocity of this penetrator is about 255 m/s higher than the penetrator initiated by TNT, and about 115 m/s lower than the velocity of the penetrator initiated by octogen.

Table 2 compares the results for 3 EFP configurations with identical characteristics and different explosive charges. It can be easily seen from the table that a higher density of explosive guarantees a higher detonation velocity, and thus a higher value of the explosive impulse transmitted from the explosive to the liner. All previously mentioned penetrator velocities are measured after 100  $\mu$ s from the initiation time point. [8]

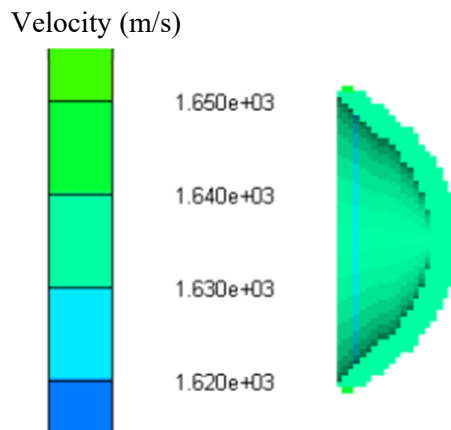


Figure 11. Penetrator velocity of EFP initiated by composition B, measured after 100  $\mu$ s (Autodyn) [8]

Table 2. Comparison of simulation parameters with different explosive charges [8]

Simulation No.	Exp. charge	Charge density (kg/m <sup>3</sup> )	Det. velocity (m/s)	Penetrator velocity (m/s)	Rel. diff. compared to TNT (%)
1	HMX	1890	9110	1750	26.8
2	TNT	1630	6940	1380	-
3	Comp.B	1720	7620	1635	18.5

Through the development of these projectiles, the charge with TNT itself was suppressed at the expense of more explosive mixtures with higher detonation velocities. This improvement leads to higher velocities and an increase in the slenderness of the penetrator, which increases its penetration capability. [8]

### 3.3. Metal liner

In order to show the influence of the liner material on the penetrating capability of the EFP, a series of numerical simulations is presented below. The basic geometry of the EFP used in the simulations is shown in Figure 5.

In this chapter the material of the liner will be varied - for the purpose of collecting information on the behavior of the explosive-formed penetrator depending on the liner material. Copper, aluminum, tantalum and iron will be used as the liner materials. After the material, the configuration and the thickness of the liner (made of copper) will also be analyzed. [8]

The first material to be used in the simulation is aluminum, the characteristics of the aluminum used in the simulation are shown in Figure 12. [8]

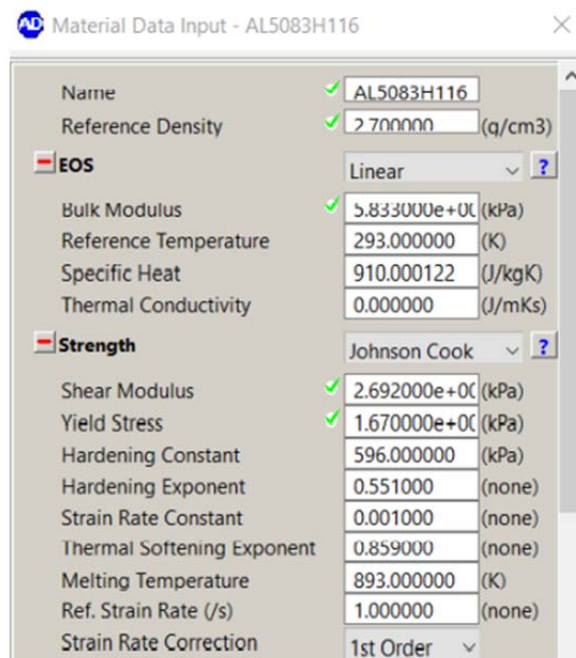


Figure 12. Characteristics of aluminum used in numerical simulation (Autodyn) [8]

Aluminum is a material of relatively low density ( $2700 \text{ kg/m}^3$ ); precisely because of its low density, the aluminum penetrator accelerates to high velocities (3500 m/s) in a short time interval. Figure 13 (left) shows the velocity of aluminum penetrator after  $30 \mu\text{s}$ , and on the right after  $50 \mu\text{s}$ . The velocity of the aluminum penetrator in both cases is about 3500 m/s. [8]

In the figure on the right, it can be noticed that the penetrator is slowly tearing apart; the reason for that is the relatively low density of aluminum. This type of aluminum penetrator is not effective in the case of firing at targets located at a greater distance, unless the thickness of the liner is increased - in this case it is 2 mm, and it is constant. [8]

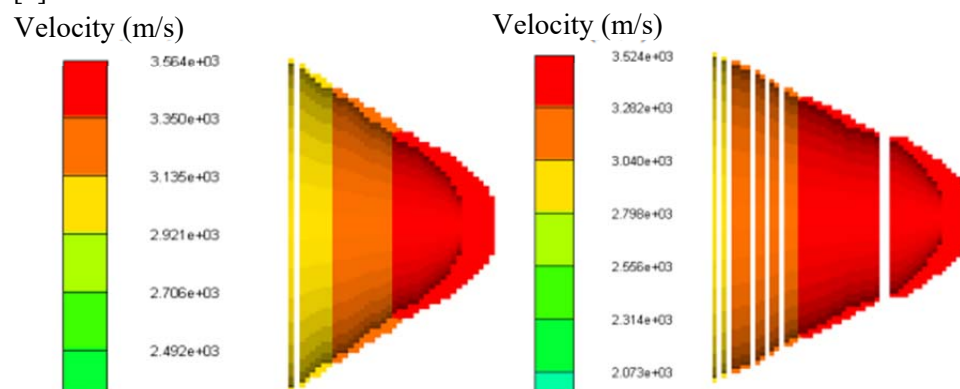


Figure 13. Velocity and shape of aluminum made penetrator (Autodyn); left-after  $30 \mu\text{s}$ , right-after  $50 \mu\text{s}$  [8]

The other material to be used in the simulation is tantalum, the characteristics of the tantalum used in the simulation are shown in Figure 14. [8]

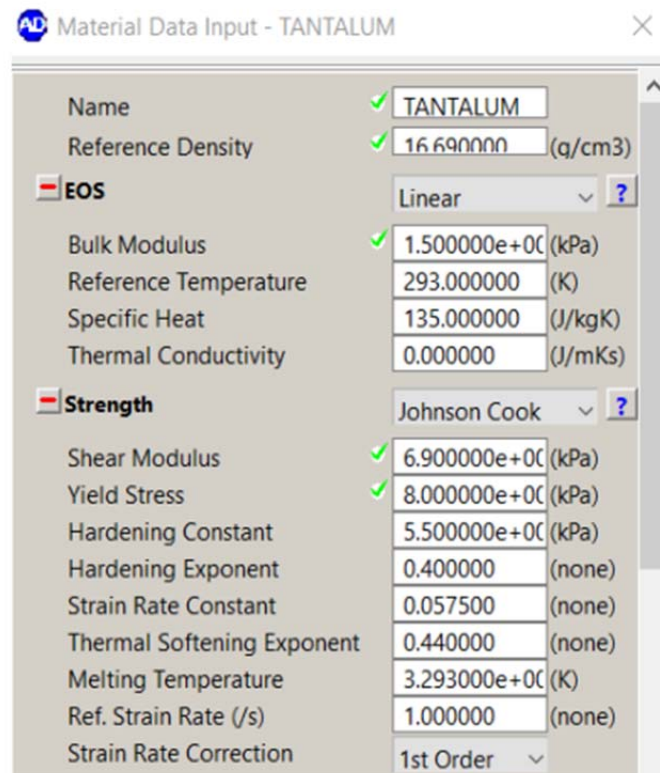


Figure 14. Characteristics of tantalum used in numerical simulation (Autodyn) [8]

Tantalum is a material of relatively high density ( $16690 \text{ kg/m}^3$ ); because of its high density, tantalum penetrator hardly accelerates to high velocities, so that the penetrator remains at lower velocities during flight compared to other tested materials. [8]

Figure 15 shows the velocity of tantalum penetrator after  $100 \mu\text{s}$ . The velocity of the penetrator is around  $1125 \text{ m/s}$ . The high density of tantalum guarantees that the penetrator barely loses its kinetic energy and is able to travel long distances. [8]

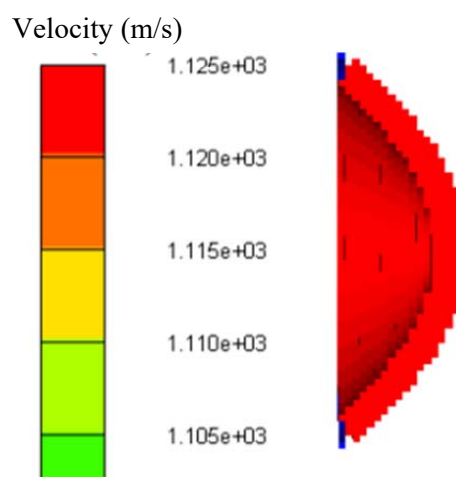


Figure 15. Velocity and shape of tantalum made penetrator (Autodyn); after  $100 \mu\text{s}$  [8]

The third material that was used in the simulation is iron, and the main characteristics of iron used in the simulation are shown in Figure 16. [8]

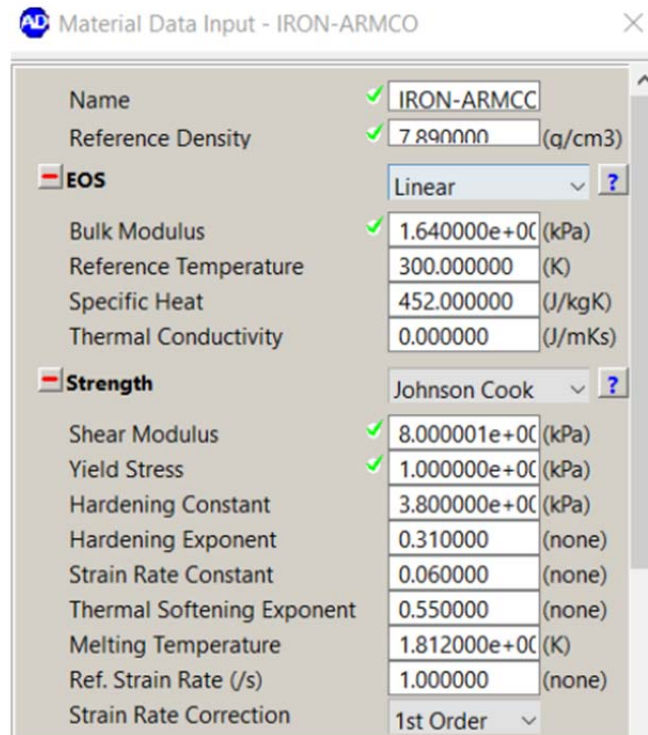


Figure 16. Characteristics of iron used in numerical simulation (Autodyn) [8]

Iron, with a density about  $7890 \text{ kg/m}^3$ , produces a penetrator with slightly higher velocity than the one made of copper. The velocity of the penetrator is around  $1882 \text{ m/s}$  (Figure 17), which is  $132 \text{ m/s}$  higher than for the copper penetrator. [8]

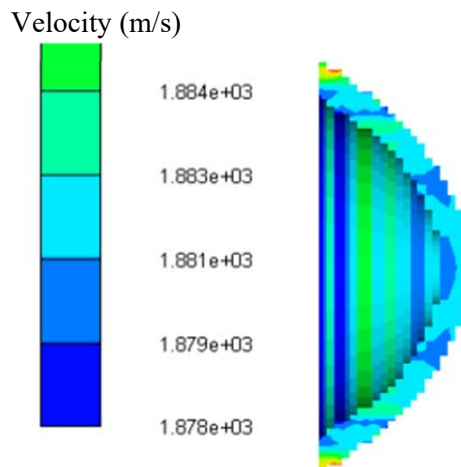


Figure 17. Velocity and shape of iron made penetrator (Autodyn); after  $100 \mu\text{s}$  [8]

Penetrator velocities are presented in Table 3.

Table 3. Comparison of penetrator velocities made of different materials [8]

Liner material	Time ( $\mu\text{s}$ )	Penetrator velocity (m/s)
Copper	100	1750
Aluminium	50	3500 - detached part
Aluminium	100	Penetrator tearing up
Tantalum	100	1125
Iron	100	1882

It can be noticed that there was a rupture of the aluminum penetrator; the detonation wave elongated aluminum penetrator way beyond its stretching limit - due to its low density and relatively weak atomic structure. The velocity and range of the tantalum penetrator are the smallest; this penetrator suffers the greatest decrease in density, which causes an increase in its temperature. Tantalum penetrator makes the largest hole (diameter) in the target (when breaking through the target, it results in a wider crater). The highest temperature occurs with tantalum penetrators - which also means the creation of hot fragments on the target. Due to its lower price, easy procurement and easy machining, iron is an attractive material for the production of EFP liners. The copper penetrator has the greatest slenderness - it is mostly used due to the greatest depth of penetration.

Copper and mild steel are the main materials used to make the liners in the EFP configuration that provide the formation of a "solid" penetrator - Figure 18 (right). Tantalum, aluminum and iron are preferred in EFP configurations that guarantee the formation of a "hollow" penetrator - Figure 18 (left). [8]

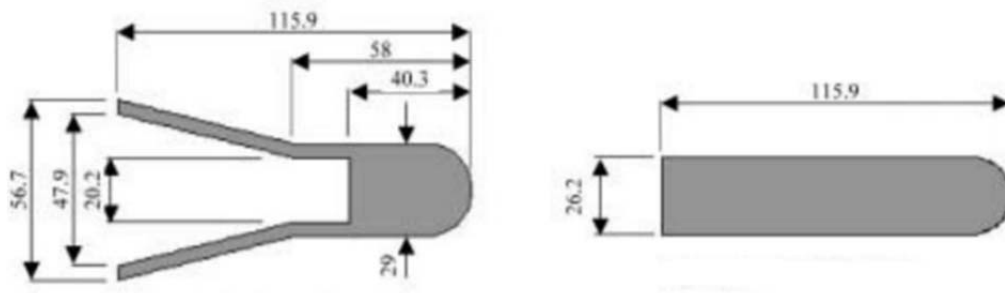


Figure 18. Hollow EF penetrator (left); Solid EF penetrator (right) [9]

In addition to the liner material, the liner geometry itself has a great influence on the penetrator formation process. The various liner shapes and penetrators formed from such shapes will be shown below.

The dependence between the geometry of the liner and the final shape of the penetrator is very complex and has not yet been adequately described. Numerical model that establishes a dependence between the finite velocity of the penetrator and the initial geometry of the liner is presented below. Two different models were used, the first model implies a constant liner thickness - the thickness in four configurations will vary from 5 to 14% of the explosive charge diameter. The second model implies variable liner thickness (thickness increases or decreases from the periphery to the center of the liner) - as presented in Table 4. Copper will be used as the liner material, as an explosive charge HMX (octogen), and detonation will be performed from the point located at the rear end of the explosive charge - on the axis of symmetry. [8]

For a constant liner thickness of 2 mm, a numerical simulation has already been presented earlier in the paper, the velocity of the penetrator was around 1750 m/s, and the mass of the liner was around 13 g. The kinetic energy of this penetrator is around 19.93 kJ, after 100  $\mu$ s. [8]

For a constant liner thickness of 3 mm, the liner mass is about 19.5 g and the penetrator velocity is around 1305 m/s (Figure 19). The kinetic energy of this penetrator, after 100  $\mu$ s is around 16.62 kJ. [8]

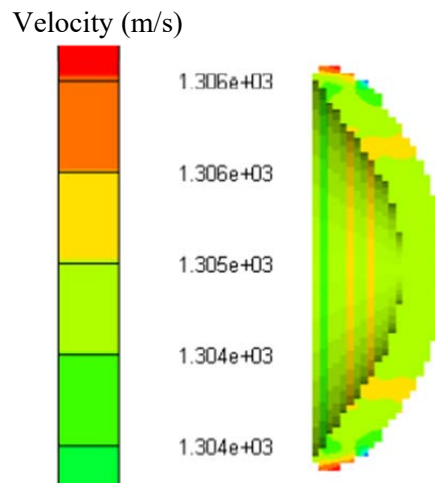


Figure 19. Velocity and shape of copper made penetrator (Autodyn); after 100  $\mu$ s (liner thickness = 3 mm) [8]

For a constant liner thickness of 4 mm, the liner mass is around 26 g and the penetrator velocity is around 1010 m/s (Figure 20). The kinetic energy of this penetrator is around 13.26 kJ. [8]

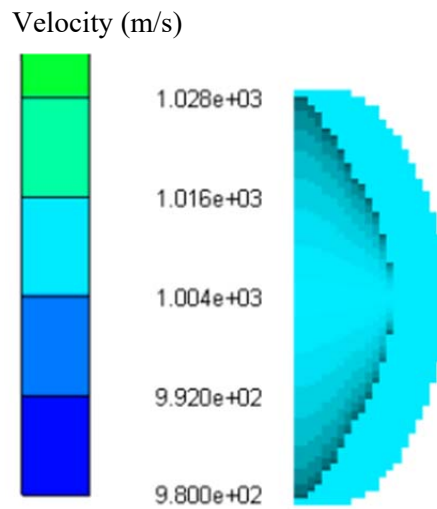


Figure 20. Velocity and shape of copper made penetrator (Autodyn); after 100  $\mu$ s (liner thickness = 4 mm) [8]

For a variable liner thickness of 2 mm in the center, and 1 mm on the periphery, the liner mass is around 9.5 g and the penetrator velocity is around 1618 m/s (Figure 21). The kinetic energy of this penetrator is around 12.45 kJ, after 100  $\mu$ s. [8]

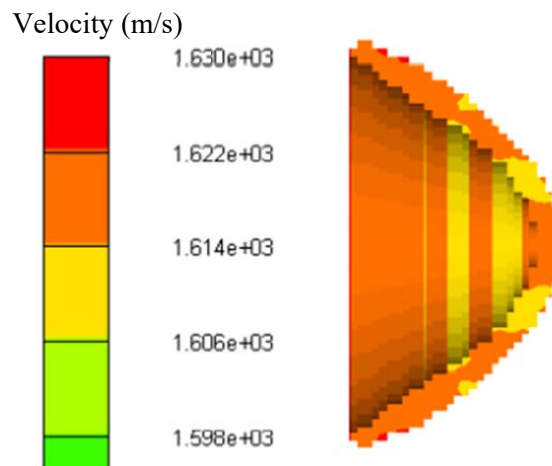


Figure 21. Velocity and shape of copper made penetrator (Autodyn); after 100  $\mu$ s – liner thickness is variable (2 mm – center; 1 mm – periphery) [8]

For a variable liner thickness of 1 mm in the center and 2 mm on the periphery, the liner mass is around 9.36 g and the penetrator velocity after 20  $\mu$ s is around 2900 m/s - the penetrator front end (Figure 22 - left). The kinetic energy of this penetrator is not relevant because it breaks.

The figure 22 on the left shows the penetrator after 20  $\mu$ s, while the figure on the right shows the penetrator after 30  $\mu$ s. It is evident that due to the velocity gradient (the velocity of the penetrators front end is about 2900 m/s and the velocity of the tail is about 1800 m/s) the penetrator will rupture - for these reasons the shaped charge jet is separated into primary and secondary jet (speaking of High-Explosive Anti-Tank warheads).

In this case, the front end of the penetrator would have the greatest impact on the penetration of the projectile - the mass of the front part of the penetrator should be calculated in order to reach the actual value of kinetic energy, assuming that no subsequent rupture of the front end of the penetrator will take place. Penetration rupture occurs solely due to the difference (variation) between the velocities of the front end and tail of the penetrator (velocity gradient). [8]

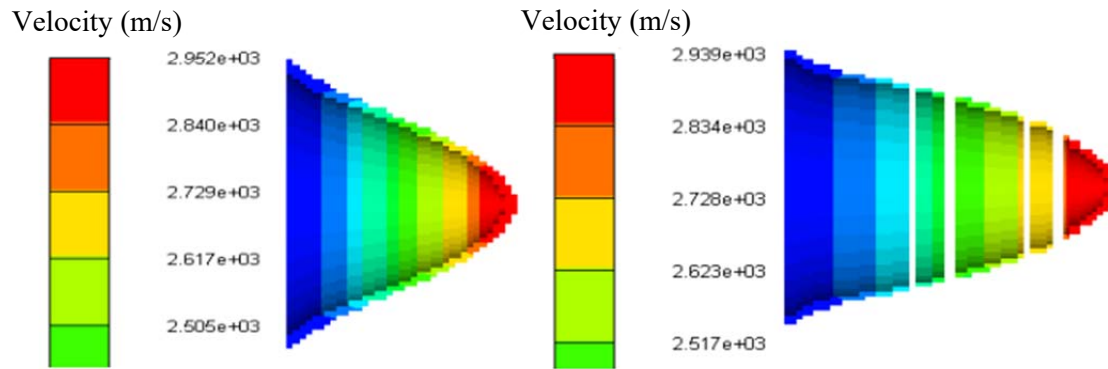


Figure 22. Velocity and shape of copper made penetrator (Autodyn); after 100  $\mu$ s – liner thickness is variable (1 mm – center; 2 mm – periphery) [8]

In the specific case, the problem was the shape of the liner. The explosive impulse first reaches the part of the liner closest to it (the central part of the liner), accelerating the central, and in this case the thinnest part of the liner to a higher velocity than the peripheral parts. Numerical simulation showed that there will be a subsequent rupture of the penetrators front end, after approximately 65  $\mu$ s, as shown in Figure 23. [8]

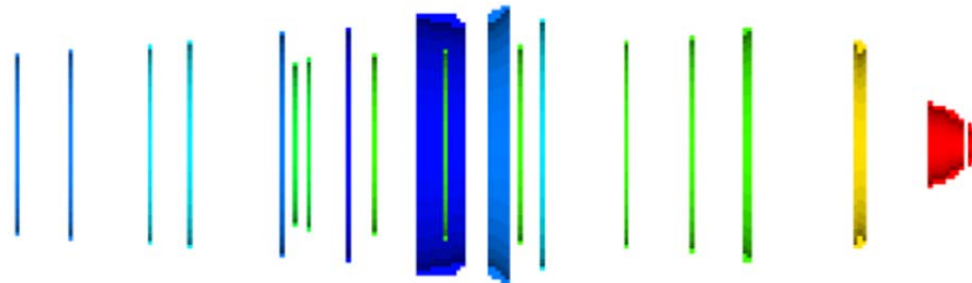


Figure 23. Copper penetrator shape (Autodyn); after 65  $\mu$ s - liner thickness is variable (1 mm center, 2 mm periphery) [8]

Table 4 presents the results of simulations where the thickness of the liner was varied to describe the behavior of the penetrator - penetrator velocities were recorded after 100  $\mu$ s, except for the velocity of 2900 m/s (after 20  $\mu$ s). [8]

Table 4. Different geometries of EFP copper made liner [8]

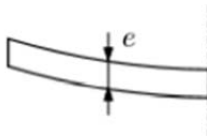
Liner configuration	Thickness	Liner mass (g)	Penetrator velocity (m/s)	Kinetic energy (kJ)
	$e = 2$ mm	13.02	1750	19.93
	$e = 3$ mm	19.52	1305	16.62
	$e = 4$ mm	26.00	1010	13.26
	$e_1 = 1$ mm	9.51	1618	12.45
	$e_2 = 2$ mm			
	$e_1 = 2$ mm	9.36	2900 – Front end	/
	$e_2 = 1$ mm			

Figure 24 shows a fully formed copper made EF penetrator after 160  $\mu$ s of simulation time. The thickness of the liner was in this case 2 mm.

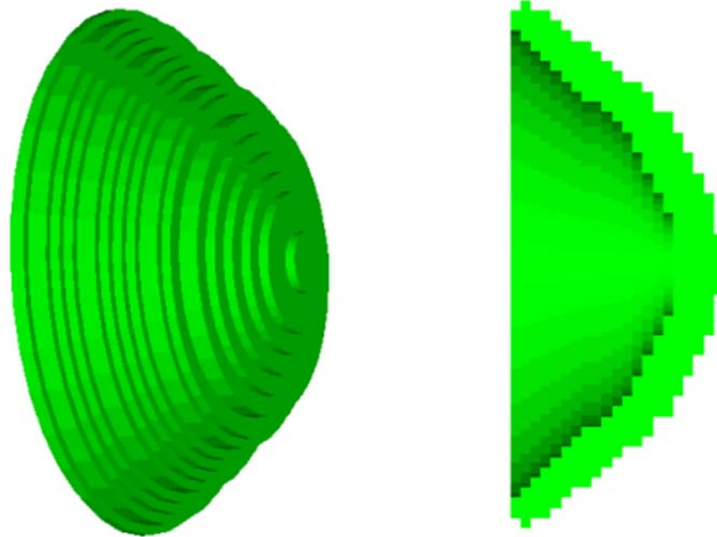


Figure 24. Fully formed copper penetrator, after 160  $\mu\text{s}$  (Autodyn) [8]

#### 4. Conclusions

Based on theoretical considerations and analysis of available numerical model (presented in [7]) for predicting the shape, velocity, pressure distribution, density and kinetic energy of explosively formed penetrator, a numerical model was created in Autodyn (ANSYS) software.

The data obtained from ref. [7] (all data obtained by numerical model presented in [7] is compared to the data obtained from experiment, and good agreement was achieved), and the data obtained by numerical simulation presented in this paper were compared. The following can be said:

1. The penetrator velocities (provided with the model from [7]) have a satisfactory agreement with the penetrator velocities from numerical model presented in this paper. The largest difference between the values is 4.12%. Maximum deviations occur when the penetrator reaches a stable velocity (while the minimum deviations occur between 10 and 40  $\mu\text{s}$  – depends on the liner material).
2. The presented numerical model gives useful results, the values of the penetrator velocity and shape. Good agreement between the results of the numerical model and experiment data indicates that the initial and boundary conditions are well set.
3. The advantage of the numerical model is that it allows the calculation of penetrators parameters based on varying the geometric, material and other characteristics of the liner, explosive and metal casing – performing relatively low-cost analysis.
4. The accuracy of the numerical model depends on the mesh, initial and boundary conditions. The accuracy of the numerical model can be increased by modifying the mesh (i.e. by increasing the number of finite elements).

## References

- [1] S. M. Zakir, L. Yulong, A. Sohail, "Numerical Study on the Optimum Design of Explosively Formed Projectile", 15th International Bhurban Conference on Applied Sciences and Technology (IBCAST), 2018.
- [2] Alan Catovic, Anti-Tank Projectiles (Lectures), Mechanical Engineering Faculty, Sarajevo, 2020.
- [3] <https://fas.org/man/dod-101/navy/docs/es310/ballstic/Ballstic.htm>,
- [4] A. Stamatovic, Projectile construction, Belgrade, 1995.
- [5] J. Carleone, Tactical Missile Warheads, Washington DC, 1993.
- [6] H. Kemmoukhe, S. Savić, S. Terzic, M. Lisov, N. Rezgui, H. Sedra, "Improvement of the Shaped Charge Jet Penetration Capability by Modifying the Liner Form Using AUTODYN-2D", Belgrade, October 2018.
- [7] G. Hussain, A. Hameed, J.G. Hetherington, A.Q. Malik, K. Sanaullah, "Analytical Performance Study of Explosively Formed Projectiles", Journal of Applied Mechanics and Technical Physics, January, 2013.
- [8] M. Salkicevic, Explosively formed projectiles, Master thesis, University of Sarajevo, Mechanical engineering faculty, Defense Technologies Department, June 2021.
- [9] F. Rondot, "Terminal Ballistics of EFPs – A Numerical Comparative Study Between Hollow and Solid Simulants 19th International Symposium of Ballistics, Interlaken, Switzerland, 7–11 May 2001.